# Analytic models for mechanotransduction: Gating a mechanosensitive channel

**Paul Wiggins\* and Rob Phillips†‡**

Divisions of *Physics, Mathematics, and Astronomy and †Engineering and Applied Science, California Institute of Technology, 1200 East California Boulevard, Pasadena, CA 91125-9500

**Analytic estimates for the forces and free energy generated by bilayer deformation reveal a compelling and intuitive model for MscL channel gating analogous to the nucleation of a second phase. We argue that the competition between hydrophobic mismatch and tension results in a surprisingly rich story that can provide both a quantitative comparison with measurements of opening tension for MscL when reconstituted in bilayers of different thickness, and qualitative insights into the function of the MscL channel and other transmembrane proteins.**

The mechanosensitive channel (MscL) is a compelling example of the interaction between a protein and the surrounding bilayer membrane. The channel is gated mechanically by membrane tension and is thought to function as an emergency relief valve in bacteria (1). MscL is a member of a growing class of proteins that have been determined to be mechanosensitive (2, 3). The dependence of the conductance on membrane tension has been studied extensively in patch-clamp experiments (4–6). In terms of the observed conductance, these studies have revealed that the channel is very nearly a two-state system. MscL spends the vast majority of its life in either a closed state (C) or an open state (O) characterized by a discrete conductance. When the bilayer tension is small, the protein is exclusively in the closed configuration. As the tension grows, the open state becomes ever more prevalent, until it dominates at high tension. The simplest structural interpretation of this conductance data is to assume that each discrete conductance corresponds to a well defined channel conformation. This assumption seems to be compatible with the conductance data. Patch-clamp experiments have also revealed that at least three additional discrete, intermediate conductance levels exist (4), suggesting three additional short-lived substates (S1–S3). Rees and coworkers (7) have solved the structure for one conformation that appears to be the open state (6, 7) by using x-ray crystallography. MscL has also been trapped in the open state (6, 8). Betanzos et al. (8) have probed the open-state structure by using disulfide crosslinking, while Perozo et al. (6) have used electron paramagnetic resonance spectroscopy (EPRS) and site-directed spin labeling (SDSL) to deduce its geometry. Sukharev et al. (9) have also proposed an open-state conformation based on structural considerations.

The conformational landscape of the MscL channel is extremely complex, depending on a huge number of microscopic degrees of freedom that are analytically intractable. Even from the standpoint of numerical calculations, this number is still very large (10). As an alternative to a detailed microscopic picture of MscL, we consider a simplified free-energy function where we divide the free energy of the system into two contributions, namely,

$$G = G_P + G_M,\qquad\qquad [1]$$

where $G_P$ is the free energy associated with the conformation of the protein and $G_M$ is the deformation free energy from the bulk of the bilayer (11). In general, these two terms are coupled. The conformation of the protein depends on the forces applied by the bilayer, while the bilayer deformation is induced by the external geometry of the protein. We denote this external geometry with a state vector, $X$, as described in more detail below. We calculate the induced bilayer deformation energy, $G_M(X)$, by minimizing the free energy of the bilayer and solving the resulting boundary value problem by using an analytic model developed for the study of bilayer mechanics (12) and protein–bilayer interactions (11, 13–15). We then apply asymptotic approximations to the exact solutions of this model for cylindrically symmetric inclusions, permitting all the results to be expressed, estimated, and understood with simple scaling relations. The advantage of this model is that it permits us to characterize the protein–bilayer system in a way that is at once analytically tractable and predictive. A wealth of useful physical intuition may be gleaned from this model, relating to both the function of MscL and that of mechanosensitive transmembrane proteins in general. Analytic estimates of the free energy generated by bilayer deformation induced by the channel reveal that these free energies are of the same order as the free-energy differences between the open and closed states measured by Sukharev et al. (4). Therefore, the mechanics of the bilayer must play an integral role in mechanotransduction and channel function. These analytic calculations reveal a compelling and intuitive model for the gating of the MscL channel that is the subject of this article. We propose that the competition between hydrophobic mismatch and applied tension, in the presence of radial constraints, generates a bistable system that is implicitly a mechanosensitive channel. Furthermore, this simple model provides a picture that is both qualitatively and quantitatively consonant with the measured dependence of the free energy on acyl chain length as observed by Perozo et al. (5). In addition, these results may also explain the stabilization of the open state by spontaneous-curvature-inducing lysophospholipids observed by Perozo et al. (5), although more experiments are required to check the consistency of this proposal.

## The Energy Landscape of the Bilayer

In the calculations considered here, the external geometry of the protein, characterized by the conformational state vector $X$, is described by three geometrical parameters $X = (R, W, H')$, where $R$ is the radius of the channel, $W$ is the hydrophobic thickness, and $H'$ is the midplane slope (see Fig. 1 for details). Although we have parameterized the conformational degrees of freedom of the protein with these three parameters in this article, we focus on the radial dependence alone, claiming that even in this reduced description, the model provides a rich variety of predictions that are compatible with previous observations and suggest other experiments. The radial dependence of the bilayer deformation energy is particularly important for MscL, because the radius undergoes a very large change between the open and closed states (9). The bilayer deformation energy

---

BIOPHYSICS
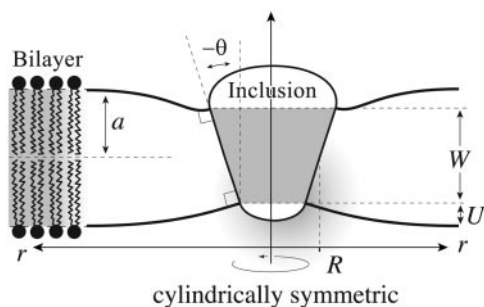
**Fig. 1.** The bilayer–inclusion model. The geometry of the inclusion is described by three parameters: $R$, the radius; $W$, the hydrophobic thickness; and $H'$, the radial midplane slope. The hydrophobic mismatch, $2U$, is the difference between the hydrophobic protein thickness, $W$, and the bilayer equilibrium thickness, $2a$. We assume the surfaces of the bilayer are locally normal to the interface of the inclusion, as depicted, implying that the midplane slope is related to the interface angle: $H' = \tan\theta$.



**Fig. 2.** The bilayer deformation energy landscape. The bilayer deformation energy is plotted as a function of the radius for different values of applied tension. The solid curves represent the bilayer deformation energy with a positive line tension, $f$, for various different tensions ($0 < \alpha_1 < \alpha_2 < \alpha_3 < \alpha_4$). The competition between interface energy and applied tension naturally gives rise to a bistable potential when the radial domain is limited by steric constraints. The gray regions represent radii inaccessible to the channel because of steric constraints. These constraints are briefly motivated in *The Energy Landscape of the Bilayer*. If the line tension is negative, depicted by the dotted curve, the potential is never bistable.

(which is derived in *Supporting Text*, which is published as supporting information on the PNAS web site) can be written explicitly in terms of the channel radius as

$$G_{\mathcal{M}} = G_0 + f \cdot 2\pi R - \alpha \cdot \pi R^2, \qquad [2]$$

where $G_0$ and $f$ do not explicitly depend on $R$ and $\alpha$ is the applied tension that triggers channel gating. $G_0$ is a radially independent contribution to the deformation energy, which is a function of the other geometrical parameters of the protein. Its importance in gating the channel is most likely secondary, because it is independent of $R$ and it will be ignored in the remainder of the discussion. The dependence of bilayer deformation energy on applied tension can be explained intuitively (3). The free-energy contribution for a small change in the channel area due to the applied tension can be written $-\alpha dA$, which is the 2D analogue of the $-PdV$ term for a gas in three dimensions. At high enough applied tension, the state with the largest inclusion area will have the lowest free energy.

The line tension, $f$, contributes an energy proportional to the circumference and is a natural consequence of the interface between two different materials. The radial dependence of line tension is linear, because the size of this interface is proportional to the circumference. In what follows, we discuss the two dominant contributions to this line tension, thickness deformation (11, 13, 14) and spontaneous curvature (15), although we note that we have treated a wide variety of other contributions (unpublished data). The thickness deformation free energy is induced by the mismatch between the equilibrium thickness of the bilayer and the hydrophobic thickness of the protein. The importance of this hydrophobic mismatch in the function of transmembrane proteins has already been established (16). The bilayer deforms locally to reduce the mismatch with the protein as shown in Fig. 1. Symbolically the thickness deformation energy (11) is

$$G_{\mathrm{U}} = f_{\mathrm{U}} \cdot 2\pi R = \frac{1}{2}\mathcal{K}U^2 \cdot 2\pi R, \qquad [3]$$

and is derived in *Supporting Text*, where $\mathcal{K} = 2 \times 10^{-2}\ kT \cdot \text{Å}^{-3}$ is an effective elastic modulus and is roughly independent of acyl chain length and $U$ is half the hydrophobic mismatch as defined in Fig. 1. Naturally, the energetic penalty for this deformation is proportional to the mismatch squared, because the minimum energy state corresponds to zero mismatch. The area of the part of the bilayer that is deformed is roughly equal to the circumference of the channel times an elastic decay length. As a result, the contribution of thickness deformation to the total free-

energy budget scales with the radial dimension of the channel. Note also that the thickness deformation free energy is always positive.

In contrast, the free energy induced by spontaneous curvature can be either negative or positive. Physically, this free energy comes from locally relieving or increasing the curvature stress generated by lipids or surfactants that induce spontaneous curvature (15, 17, 18).[§] Again the radial dependence of this free energy will be linear, because the effect is localized around the interface. Because the leaflets of the bilayer can be doped independently (5), the spontaneous curvatures of the top and bottom leaflets, $C_\pm$, can be different. It is convenient to work in terms of the composite spontaneous curvature of the bilayer, $C \equiv \frac{1}{2}(C_+ - C_-)$. The contribution to the deformation energy arising from spontaneous curvature is given by (15)

$$G_{\mathrm{C}} = f_{\mathrm{C}} \cdot 2\pi R = K_{\mathrm{B}}CH' \cdot 2\pi R, \qquad [4]$$

and is derived in *Supporting Text*, where $H'$ is the midplane slope and $K_{\mathrm{B}} = 20(a/20\ \text{Å})^3\ kT$, is the bending modulus, which roughly scales as the third power of the bilayer thickness. Notice that if $C$ and $H'$ have opposite signs, the deformation energy and the corresponding line tension, $f_{\mathrm{C}}$, will be negative. We note that the elastic theory of membrane deformations associated with proteins like MscL permit other terms (such as midplane deformation, for example) which can be treated within the same framework and give rise to the same radial dependence as that described here. However, for the purposes of characterizing the energetics of MscL, these other terms are less important than the two considered here.

Typically, in the absence of large spontaneous curvature, the line tension, $f$, will be dominated by the mismatch and will be positive. A potential of the form described by Eq. **2** is depicted schematically in Fig. 2. In this figure, we have implied that steric

---

[§]When discussing the lipids used by other authors, we have used the same naming convention as they used: 10:0 dicaproyl-phosphatidylcholine (PC10), 12:0 dilauroyl-phosphatidylcholine (PC12), 14:1 dimirstoyl-phosphatidylcholine (PC14), 16:1 dipalmito-leoyl-phosphatidylcholine (PC16), 18:1 dioleoyl-phosphatidylcholine (PC18), 20:1 eicos-senoyl-phosphatidylcholine (PC20), lysophospholipid (LPL), lysophosphatidylcholine (LPC), and dioleoyl-phosphatidylethanolamine.

Wiggins and Phillips

constraints exist for the range of radii accessible to the protein. Assuming that the radius of the inclusion has a lower bound is very natural. It can be understood as the radius below which the residues begin to overlap. This steric constraint will generate a hard wall in the protein conformation energy, forbidding lower radii. Similar but slightly more elaborate arguments can made for an upper bound. The bilayer deformation energy generates a barrier between small-radius and large-radius states. The location of the peak of this barrier is the turning point, $R_* \equiv f/\alpha$. At small tension, the turning point is very large and is irrelevant because it occurs at a radius not attainable by the channel due to the steric constraints, but, as the tension increases, the position of the turning point decreases. This behavior is reminiscent of the competition between surface tension and energy density for nucleation processes that gives rise to a similar barrier (e.g., ref. 19).

Although the conformational landscape of the MscL channel is certainly very complicated, an intriguing possibility is that the channel harnesses the elastic properties of the bilayer, which quite naturally provide the properties we desire in a mechanosensitive channel: a stable closed state at low tension and a stable open state at high tension. In effect, we will treat the bilayer deformation energy as an external potential with respect to the conformational energy landscape of the protein. The physical effects of the radial dependence of the bilayer deformation energy on the inclusion conformation can be recast in a more intuitive form by appealing to the induced tension that accounts not only for the applied far-field tension, but also for *induced* tension terms due to bilayer deformation. The applied tension is not the whole story! The generalized forces are obtained by differentiating the bilayer deformation energy with respect to bilayer excursions. The net tension induced by the bilayer on the inclusion interface is

$$\alpha_\Sigma = \alpha - \frac{f}{R},$$ **[5]**

where we have denoted the net tension $\alpha_\Sigma$ because we have already used $\alpha$ to denote the applied tension. For radii smaller than the turning point, $R_*$, the bilayer deformation energy is an increasing function of radius and, therefore, the net tension is negative and acts to compress the channel, which we refer to as compressive tension. For radii larger than that at the turning point, the bilayer deformation energy is a decreasing function of radius and the net tension is positive and acts to expand the channel. The combination of these constraints and the bilayer deformation energy lead to a bistable system where the closed and open states correspond to the constraint-induced radial minimum and maximum, respectively. Recall that the net tension on the closed state will be compressive as long as its radius is smaller than that at the turning point, namely, $R_C < R_*$. This inequality defines the range of applied tension over which the closed state is stabilized by the bilayer deformation energy. The net tension on the open state will be expansive as long as its radius is greater than that at the turning point: $R_O > R_*$. This inequality defines the range of applied tension over which the open state is stabilized by the bilayer deformation energy. An intermediate range of tensions exists for which both states are stabilized by the bilayer: $f/R_O < \alpha < f/R_C$. The bilayer deformation energy naturally destabilizes the open state for applied tension below this range while stabilizing the closed state for applied tensions up to the limit of this range. Both effects help to prevent the channel from leaking at low applied tension. This bistability is precisely the desirable behavior for a mechanosensitive channel designed to relieve internal pressure, and yet surprisingly little is required from the protein conformational landscape, $G_P$, except for steric constraints that arise very naturally. In Fig. 3, we have depicted the way in which MscL
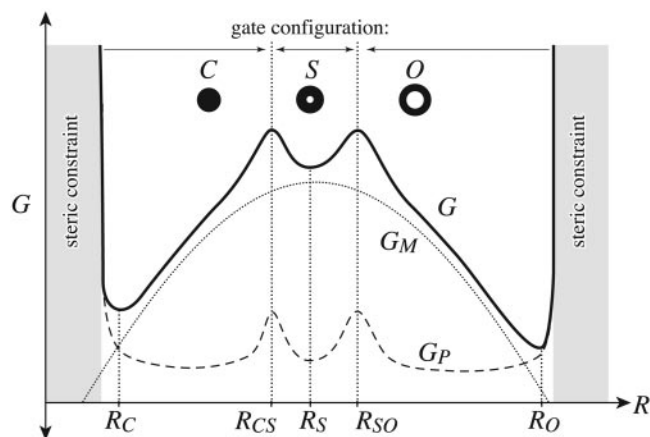


**Fig. 3.** The total free energy. The total free energy, $G$, of the protein and bilayer are plotted schematically as a function of channel radius. The bilayer deformation energy, $G_M$, is represented by the dotted curve. A protein conformation energy is represented schematically by the dashed curve. Their sum gives the total free energy $G$. The protein energy has been chosen to contain a single substate, $S$. A conformational energy barrier is shown that corresponds to changing the gate conformation of the channel. These transitions occur at $R_{CS}$ and $R_{SO}$. $G_P$ also contains steep barriers corresponding to steric constraints. The radii of the conductance states are defined by the free-energy minima of $G$.

mimics this mechanical analogue by using the sum of a schematic protein energy and the bilayer deformation energy to form energy minima corresponding to the open and closed states.

Our discussion of the role of the bilayer enables us to make some general observations about the nature of the substates. To generate a substate, we assume that more than one gating transition occurs in the protein conformational energy. One gating transition would correspond to a closed-to-open transition. An additional gating transition allows three conductance states. We will assume that these transitions are themselves bistable in nature, because the conductance data would seem to imply the lifetimes of the transition states are very short compared with the conductance states (4). In other words, the conformational gating transition occurs near a local maximum in the conformational free energy. If we add two such transitions to $G_P$, we generate a substate of intermediate radius between these two transition-state radii. A schematic example of this is illustrated in Fig. 3. Sukharev *et al.* (4) have shown that all the substates are short-lived and have estimated the areas of each state based on the tension dependence of their free energies. [Evidence is now available for additional substates (20).] Specifically, they have shown that the radii of the substates lie between the open- and closed-state radii. If the bilayer deformation dominates the free energy of the states, the ephemeral nature of the substates is a natural consequence of their intermediate radii. The compressive tension due to the mismatch stabilizes the state of lowest radius at low applied tension. At high applied tension the bilayer stabilizes the state with highest radius. All the states with intermediate radii are never stabilized by the bilayer and are therefore short-lived. Our deceptively simple mismatch model quite naturally leads to short-lived substates at intermediate radii.

## Results

The patch-clamp experiments of Perozo *et al.* (5) go beyond the earlier work of Sukharev *et al.* (4) by providing experimental values for the free-energy difference between the open and closed states for bilayers of several thicknesses. These results can be compared with our predictions. To apply our model, we must

determine the geometrical parameters of the state vector $X$ for the open and closed states and, in particular, the open and closed radii. The radius of the closed state is known from x-ray crystallography (7): $R_C \sim 23$ Å. Structural studies (9) and EPRS and SDSL (6) experiments have suggested an open-state radius of roughly $R_O \sim 35$ Å. To estimate the line tension and free energy generated by hydrophobic mismatch, we must determine the hydrophobic thickness $W$. (We ignore the difference in hydrophobic thickness between the open and closed states.) In principle, one might have thought this could be deduced from the atomic-level structure of MscL, but in practice, real structures are complicated, often lacking a clear transition from hydrophobic to hydrophilic residues on the interface. However, this width may be deduced from the EPRS and SDSL data of Perozo et al. (5). EPRS and SDSL experiments measure intersubunit proximity and spin-label mobility, respectively (5). Compressive tension in the bilayer suppresses the fluctuations of the protein, increasing the subunit proximity and reducing the spin-label mobility. In the experiments of Perozo et al. (5), the applied tension is low, implying that the net tension is dominated by the line tension, induced by thickness deformation ($\alpha_\Sigma \sim -\hat{\mathcal{K}}U^2/2R$), in the absence of spontaneous curvature. This tension is compressive and proportional to the mismatch squared. Therefore, when the mismatch is zero, the tension reaches a minimum, implying that mobility and subunit separation should reach a maximum. The EPRS and SDSL data of Perozo et al. (5) may turn over for PC12 bilayers, implying that the mismatch is zero, which would imply, in turn, that $W \sim 2a_{n=12}$, but because of the quadratic dependence on $U$, the slope in the vicinity of the turnover is small. Because PC lipids with acyl chain lengths shorter than $n = 10$ do not form stable bilayers (5), it is difficult to extensively check the quadratic dependence on $U$. The predicted turnover would be more pronounced for PC bilayers with $n < 10$. We shall see that this deduced hydrophobic mismatch is compatible with the patch-clamp measurements of Perozo et al. (5). However, the interpretation of these EPRS data becomes more complicated when the thickness of the channel changes between the open and the closed state as discussed in *Discussion*.

Perozo et al. (5) have measured $\Delta G_0$, the free-energy difference between the open and closed state at zero tension for three acyl chain lengths. [The free energy measured by Perozo et al. (5) is equivalent to the free energy at zero tension modulo several assumptions (3).] Using the value we have deduced for $W$, we can now calculate the free-energy difference between the open and closed states due to bilayer deformation at zero tension, $\Delta G_{0,\mathcal{M}}$, which is given by the line tension contribution alone as $\Delta G_{0,\mathcal{M}} = f 2\pi \Delta R \to f_U 2\pi \Delta R$, where $\Delta R$ is the difference between the open and closed radii. The theoretical result, $\Delta G_{0,\mathcal{M}}$, is plotted with the experimental measurements of $\Delta G_0$ in Fig. 4. The agreement between experiment and theory is embarrassingly good given the simple fashion in which we have chosen the geometrical parameters and that we have neglected the protein conformational energy, $G_P$, entirely. A very important point can be made about these results. Perozo et al. (5) measured three data points and our model is quadratic, implying that we could have chosen the parameters of our model to fit the data points perfectly because any three points lie on a parabola, but our parameters have, in fact, been deduced independently rather than fit, which is why this correspondence with the data is remarkable. This model corresponds to a channel where the free-energy difference between the open and closed states is dominated by the bilayer deformation rather than protein conformation. Our model implies that $\Delta G_0$ for PC10, PC12, and PC14 should be very small. Unfortunately these bilayers have proved too weak for patch-clamp measurements of $\Delta G_0$ (5). Certainly none of these bilayers trap the channel in the open state (5).
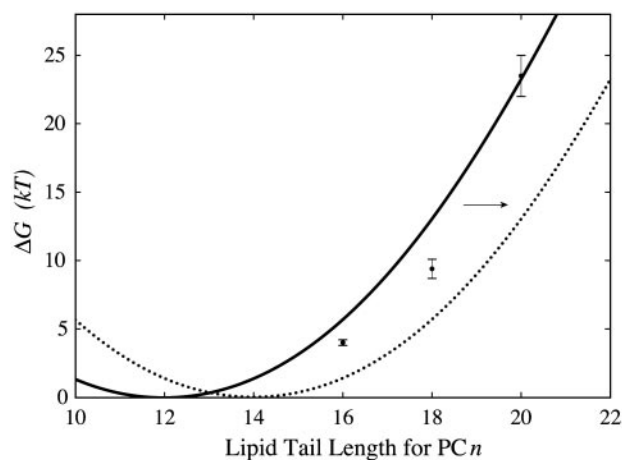


**Fig. 4.** The free-energy difference between open and closed states vs. lipid acyl chain length. The experimental data of Perozo et al. (5) for the free-energy difference between the open and closed states at zero tension, $\Delta G_0$, is plotted with black circles and error bars. The solid curve represents the theoretical values for the bilayer deformation energy generated by a simple thickness-deformation model at zero tension, $\Delta G_{0,\mathcal{M}}$. The dotted curve represents the translated $\Delta G_{0,\mathcal{M}}$ for an engineered MscL channel with a hydrophobic thickness matching a PC14 bilayer.

The opening tension is defined as the tension at which the open and closed state probabilities are equal or, analogously, the tension at which the free energies of the open and closed states are equal. The opening tension is

$$\alpha_{1/2} = \frac{f}{\bar{R}} + \frac{\Delta G_P}{\Delta A}, \qquad [6]$$

where $\bar{R} \equiv \frac{1}{2}(R_C + R_O)$ is the mean radius, $\Delta G_P$ is the difference in the open and closed state protein conformation energy, and $\Delta A$ is the difference in open and closed state area. When the bilayer deformation energy dominates, the opening tension is determined by the first term alone. Changing the sensitivity of the channel is straightforward from this perspective. Changes in the length of the hydrophobic region of the protein can increase or decrease the opening tension of the channel. For example, MscL channels might be engineered with an expanded hydrophobic region that matches PC14 bilayers. Our mismatch-based theory would predict that the free energy versus acyl chain length curve would simply be translated to higher $n$ so that the minimum $\Delta G_{0,\mathcal{M}}$ is realized for a PC14 bilayer. This shift should be measurable, reducing $\Delta G_0$ for PC16, PC18, and PC20 bilayers. The reduction in mismatch may also allow MscL to be reconstituted into PC22 bilayers, allowing an additional data point. The proposed shift should also be measurable in EPRS and SDSL measurements of residue proximity and mobility. The maximum mobility and separation should now be centered at about $n = 14$, perhaps permitting a clear measurement of the rise in induced tension for a PC10 bilayer predicted by the quadratic dependence of the line tension on the mismatch.

Perozo et al. (5) have proposed that asymmetric bilayer stresses play a central role in MscL gating. They have proposed this model based on patch-clamp, EPRS, and SDSL experiments showing that spontaneous curvature can induce MscL channel opening. Specifically, they find that MscL reconstituted into PC vesicles with high enough concentrations of asymmetrically incorporated lysophosphatidylcholine (LPC) stabilizes the open state of the channel, whereas MscL reconstituted into PC vesicles with symmetrically incorporated LPC does not stabilize the open state. Unlike Keller et al. (21), Perozo et al. have measured neither the spontaneous curvature for the mixed bilayer nor the

free-energy difference between open and closed states as a function of LPC concentration. In the absence of these quantitative experimental results, it is difficult to make concrete comparisons between our model and the experimental data. For large spontaneous curvature (21) but a relatively modest complementary midplane slope, the free energy difference between the two states due to spontaneous curvature is

$$\Delta G_C \sim 2\pi(R_O - R_C)K_B CH' = -16\left(\frac{20\,\text{Å}}{C^{-1}}\right)\left(\frac{H'}{-0.2}\right)kT,$$

$$[7]$$

an energy typically large enough to stabilize the open state. In *The Energy Landscape of the Bilayer*, we have made some rather general arguments about the shape of the bilayer deformation energy landscape. We now return to this picture briefly to discuss the consequences of spontaneous curvature. In our discussion, we assumed that the line tension, $f$, was typically positive, but we remarked that this need not be the case in the presence of a large spontaneous curvature. If $f$ is negative, as depicted by the dotted curve in Fig. 2, the only state stabilized by the bilayer is the open state, which very naturally gives rise to the open-state stabilization observed by Perozo *et al.* (5). Alternatively, this result can be understood from the predicted opening tension in Eq. **6**. When $\Delta G_0$ is bilayer deformation dominated, a negative $f$ implies that the opening tension is itself negative! A compressive force is required to stabilize the closed state. This argument gives a tantalizingly simple explanation for the open-state stabilization but, in the absence of measured values for the spontaneous curvature induced by LPC, we can only conclude that spontaneous curvature can stabilize the open states for rather generic values of the parameters. An experimental consistency check of these results is fairly simple. Perozo *et al.* have incorporated LPC asymmetrically. The same experiment might be repeated with $H_{II}$ phase-inducing lipids, which can also be used to generate spontaneous curvature but of the opposite sign. For the dioleoyl-phosphatidylcholine/dioleoyl-phosphatidylethanolamine system of Keller *et al.* (21), the spontaneous curvature is known and tunable as a function of concentration. Our results predict that $\Delta G_0$ should be linear in $C$ (15) and compatible with Eq. **7**.

In the argument above, we focused on the radial dependence of bilayer deformation free energy and fixed the other components of the state vector, $X$. In principle, we are missing a potentially important piece of radial dependence. The internal conformation may effectively couple the radius to the other parameters in the state vector $X$, adding additional implicit radial dependence. For example, the thickness of the inclusion, $W$, is almost certainly a function of radius. It is also natural to couple the midplane slope to the radius. We have ignored these dependences to develop an intuitive and simple 1D picture with as few undetermined constants and couplings as possible. Provided that the bilayer deformation energy change is dominated by the radial change, this simplified model is a useful tool for understanding the bilayer-inclusion interaction. More elaborate models might easily be built from the general analytic framework we have constructed. This framework will be described in a forthcoming paper.

## Discussion

We have argued that the bilayer deformation energy is harnessed by MscL to govern channel gating. Indeed, we have shown that a model that attributes the entire free-energy difference between the open and closed states to the bilayer deformation energy is compatible with the experimental data. These results are somewhat surprising, because it has been shown experimentally that the mutation of a single residue in the vicinity of the channel gate can significantly affect channel gating (22, 23). The protein

conformational energy cannot be neglected in general. In fact, we have assumed that the protein conformational energy is large enough to constrain the channel geometry because we have assumed it is the bilayer that deforms rather than the protein. In principle, the closed state could have been stabilized by protein conformation alone, rather than mismatch, but exploiting bilayer deformation provides a robust mechanism for mechanotransduction, a design principle that functions despite the enormous number of nearly degenerate microstates endemic to proteins. Even for proteins as simple as myoglobin, Frauenfelder *et al.* (24) have shown that the macroscopic conformation corresponds to an enormous number of structurally distinct microstates. These ideas have already been exploited for channel proteins. Goychuk and Hänggi (25) have used this degenerate landscape to derive the empirical rate law for voltage-gated channels. In light of these results, it is natural to suppose that the protein conformational energy of the MscL protein gives rise to a vast number of nearly degenerate states as well. The bilayer deformation energy naturally breaks this degeneracy and forms a mechanotransducing channel. The ensemble of microstates we observe as the closed states is stabilized at low applied tension by the line tension, whereas the ensemble of microstates we observe as the open state is stabilized by high applied tension. The importance of bilayer deformation in mechanotransduction may help to explain why no obvious sequence motifs are associated with mechanosensitivity (26), because a mismatch requirement does not imply sequence specificity. Harnessing bilayer elasticity does have one noted disadvantage. The gating of a channel will be affected by the membrane environment that surrounds it. This effect is precisely what the experiments of Perozo *et al.* (5) showed. In realistic cell membranes, the enormous diversity of proteins and lipids would imply that the free energy and, therefore, opening tension in these membranes is heterogeneous. Sukharev and coworkers (20) have evidence for exactly this variability for MscL in giant spheroplasts.

The reader may be concerned that we are attempting to invalidate the structural models of Betanzos *et al.* (8), Sukharev *et al.* (9), Perozo *et al.* (6), and other investigators of the MscL channel. This could not be further from the truth. Indeed much of the input to our model comes from these investigations. Our aim is rather to model the physical principles (5) that have been proposed with a simple, self-consistent model for channel–membrane interaction. An objection to our model as proposed above is that we do not account for the change in the hydrophobic thickness from closed to open state. Indeed, it is difficult to envision a consistent atomic-scale model where the thickness of the channel is not reduced as the radius is increased. Furthermore, data from Betanzos *et al.* (8), Perozo *et al.* (6), and new data from Powl *et al.* (27) suggest that this added complexity is probably more experimentally accurate. Although these more detailed considerations complicate the story theoretically, they do not significantly change the energetic results of the model (unpublished data). The failure of our model to predict the same zero mismatch lipid length for the closed state as Powl *et al.* (27) is a consequence of the choice of one channel thickness for both states. The price of the clarity and simplicity of our coarse-grained model is an insensitivity to the degrees of freedom we ignore. For the sake of brevity in this article, we have focused on the physical mechanism we believe to be most essential to understanding the MscL channel mechanics.

The correspondence between our simple theoretical model for the gating of the MscL channel and experiment at least strongly suggests that this mechanism is exploited by the MscL channel. Our model can also naturally explain the stabilization of the open state by LPC (5) and the ephemeral nature of the substates (4). The tractable nature and simplicity of the model allow extensive analytic calculations to be made, which have in turn led to numerous experimental predictions, discussed in *Results*.

Specifically, we have predicted (*i*) a shift in the curve relating the free-energy difference and acyl chain length when the hydrophobic thickness of the channel is altered and (*ii*) the dependence of the free energy on spontaneous curvature and, in particular, on the concentration of spontaneous curvature-inducing molecules.

We have developed a framework for studying bilayer–inclusion interactions in the MscL system. The model we have discussed here is the simplest implementation of these results. The current work has several very natural extensions. For example, we have focused here on the radial dependence only, but, as we have briefly alluded to in *Results*, two additional geometric parameters may also play important roles in the function of the MscL channel. More detailed measurements of the rates and free energies of the various states will no doubt prove that our simplified model is incomplete and provide motivation and insight into a more detailed model of channel gating. The simplicity and generality of the competition between applied tension and a line tension, regardless of its source, suggests that it may be a quite general phenomenon for mechanotransduction. We hope to apply similar ideas to other mechanosensitive systems. More generally, we are also intrigued by the possibility of finding analogous bilayer-deformation-driven conformational changes for other transmembrane proteins that do not exhibit mechanosensitive function, perhaps illuminating a more general qualitative design principle for the function of transmembrane proteins.

1. Blount, P. & Moe, P. C. (1999) *Trends Microbiol.* **7,** 420–424.
2. Gillespie, P. G. & Walker, R. G. (2001) *Nature* **413,** 194–202.
3. Sachs, F. (1992) *Soc. Gen. Physiol. Ser.* **47,** 241–260.
4. Sukharev, S. I., Sigurdson, W. J., Kung, C. & Sachs, F. (1999) *J. Gen. Physiol.* **113,** 525–539.
5. Perozo, E., Kloda, A., Marien Cortes, D. & Martinac, B. (2002) *Nat. Struct. Biol.* **9,** 696–703.
6. Perozo, E., Kloda, A., Marien Cortes, D. & Martinac, B. (2002) *Nature* **418,** 942–948.
7. Chang, G., Spencer, R. H., Lee, A. T., Barclay, M. T. & Rees, D. C. (1998) *Science* **282,** 2220–2226.
8. Betanzos, M., Chiang, C.-S., Guy, H. R. & Sukharev, S. (2002) *Nat. Struct. Biol.* **9,** 704–710.
9. Sukharev, S. I., Durell, S. R. & Guy, H. R. (2001) *Biophys. J.* **81,** 917–936.
10. Gullingsrud, J. & Schulten, K. (2003) *Biophys. J.* **85,** 2087–2099.
11. Huang, H. W. (1986) *Biophys. J.* **50,** 1061–1070.
12. Helfrich, W. (1973) *Z. Naturforsch. C* **28,** 693–703.
13. Nielsen, C., Goulian, M. & Andersen, O. (1998) *Biophys. J.* **74,** 1966–1983.
14. Goulian, M., Mesquita, O. N., Fygenson, D. K., Nielsen, C., Andersen, O. S. & Libchaber, A. (1998) *Biophys. J.* **74,** 328–337.
15. Dan, N. & Safran, S. A. (1998) *Biophys. J.* **75,** 1410–1414.
16. Killian, J. A. (1998) *Biochim. Biophys. Acta* **1376,** 401–416.
17. Israelachvili, J. N. (1991) *Intermolecular and Surface Forces* (Academic, London), 2nd Ed.
18. Gruner, S. M. (1989) *J. Phys. Chem.* **93,** 7562–7570.
19. Kittel, C. & Kroemer, H. (1980) *Thermal Physics* (Freeman, New York), 2nd Ed.
20. Chiang, C. S., Anishkin, A. & Sukharev, S., *Biophys. J.*, in press.
21. Keller, S. L., Bezrukov, S. M., Gruner, S. M., Tate, M. W. & Vodyanoy, I. (1993) *Biophys. J.* **65,** 23–27.
22. Ou, X., Blount, P., Hoffman, R. J. & Kung, C. (1998) *Proc. Natl. Acad. Sci. USA* **95,** 11471–11475.
23. Yoshimura, K., Batiza, A., Schroeder, M., Blount, P. & Kung, C. (1999) *Biophys. J.* **77,** 1960–1972.
24. Frauenfelder, H., Sligar, S. G. & Wolynes, P. G. (1991) *Science* **254,** 1598–1603.
25. Goychuk, I. & Hänggi, P. (2002) *Proc. Natl. Acad. Sci. USA* **99,** 3552–3556.
26. Strop, P., Bass, R. & Rees, D. C. (2003) *Adv. Protein Chem.* **63,** 177–209.
27. Powl, A. M., East, J. E. & Lee, A. G. (2003) *Biochemistry* **42,** 14306–14317.